PROCEEDINGS OF SCIENCE

Leptoquark and vectorlike quark extended models as the explanation of $(g-2)_\mu$ anomaly

Shi-Ping He[a,*]

[a]*Asia Pacific Center for Theoretical Physics, Pohang 37673, Korea*

E-mail: shiping.he@apctp.org

In minimal leptoquark (LQ) models, the R_2 and S_1 can be the solution to the $(g-2)_\mu$ anomaly because of the chiral enhancements. Here, we study the LQ and vectorlike quark (VLQ) extended models. In the one LQ and one VLQ extended models, the $(g-2)_\mu$ can receive the contributions from top and top partner T because of the $t-T$ mixing. Besides the traditional R_2 and S_1 representations, we find that the S_3 LQ can also explain the anomaly when including the $(X,T,B)_{L,R}$ triplet at the same time. Moreover, we find that the LQ has the new decay channel $T\mu$ in these models.

41st International Conference on High Energy physics - ICHEP2022
6-13 July, 2022
Bologna, Italy

*Speaker

PoS(ICHEP2022)137

1. Introduction

The muon magnetic moment is well predicted in the standard model (SM) of elementary particle physics, and the most accurate calculation is $a_\mu^{\rm SM} = 116591810(43)\times 10^{-11}$ [1]. Its deviation from the SM prediction can be a good probe to new physics. The $(g-2)_\mu$ anomaly is first reported by the E821 experiment at BNL [2]. Last year, the FNAL muon $g-2$ experiment announces the average result $a_\mu^{\rm Exp} = 116592061(41)\times 10^{-11}$ after combining the BNL and FNAL data [3], which shows the 4.2σ discrepancy with $\Delta a_\mu \equiv a_\mu^{\rm Exp} - a_\mu^{\rm SM} = (251\pm 59)\times 10^{-11}$. There are many interpretations on this anomaly regardless of theoretical and experimental uncertainties, or new physics. In our paper [4], we propose the simultaneous scalar LQ and VLQ extended models to explain this anomaly.

2. The LQ and VLQ extended models

For the mediator with mass scale Λ above TeV, we have the rough estimation $m_\mu^2/(8\pi^2\Lambda^2) \lesssim 10^{-10}$. Thus, the chiral enhancements are required to explain the $(g-2)_\mu$. In the minimal LQ models, only the R_2 and S_1 representations can lead to the left and right-handed (non-chiral) couplings to muons at the same time. In fact, the chiral enhancements are induced by the up-type quarks [5].

There are seven typical VLQs, while we are interested in the five types with top partner T [6], namely, the singlet $T_{L,R}$, doublets $(X,T)_{L,R}/(T,B)_{L,R}$, and triplets $(X,T,B)_{L,R}/(T,B,Y)_{L,R}$. Here, the X,T,B,Y quarks carry the $5/3, 2/3, -1/3, -4/3$ electric charges, respectively. Although the five scalar LQs and five T VLQs can result in twenty-five combinations totally, only some combinations can lead to the up-type quark chiral enhancements. In the following, we will study these combinations, which are named as "LQ + VLQ" [1].

After the electroweak symmetry breaking, there are $t-T$ and $b-B$ mixings with the mixing angles denoted as $\theta^t_{L,R}$ (also $\theta_{L,R}$) and $\theta^b_{L,R}$. Hereafter, the $\sin\theta_{L,R}$ and $\cos\theta_{L,R}$ will be abbreviated as $s_{L,R}$ and $c_{L,R}$ (similar to the b). For the mentioned VLQs, there is only one independent mixing angle except for the $(T,B)_{L,R}$ with two independent mixing angles θ^t_R and θ^b_R. In our paper [4], we list the relevant input parameters and mixing angle identities. For the singlet and triplet VLQs, the θ_L is chosen as the input mixing angle. For the doublet VLQs, the θ_R is chosen as the input mixing angle [6]. In Tab. 1, we parametrize the couplings in front of the $\bar{\mu}t(R_2^{5/3})^*$, $\bar{\mu}T(R_2^{5/3})^*$, $\bar{\mu}t^C(S_1)^*$, $\bar{\mu}T^C(S_1)^*$, $\bar{\mu}t^C(S_3^{1/3})^*$, and $\bar{\mu}T^C(S_3^{1/3})^*$ interactions. In Tab. 2, we also list the couplings in front of the $\bar{\mu}b(R_2^{2/3})^*$, $\bar{\mu}B(R_2^{2/3})^*$, $\bar{\mu}b^C(S_3^{4/3})^*$, and $\bar{\mu}B^C(S_3^{4/3})^*$ interactions.

3. Contributions to the $(g-2)_\mu$

In all of the mentioned models, there are top and T quark contributions with chiral enhancements. In the R_2+VLQ models, there are also b and B quark contributions. In the S_1+VLQ models, there are no b or B quark contributions. In the $R_2/S_3+(X,T,B)_{L,R}$ models, the b and B quark contributions are also chirally enhanced. For the models with X quark, the X quark only contributes in the $S_3+(X,T,B)_{L,R}$ model but without the chiral enhancements. For the $R_2/S_1+(T,B,Y)_{L,R}$ models, the Y quark does not contribute to $(g-2)_\mu$.

[1] In our paper [4], we also investigate the one LQ and two VLQ extended models.

LQ	VLQ	$\overline{\mu_R} t_L$	$\overline{\mu_L} t_R$	$\overline{\mu_R} T_L$	$\overline{\mu_L} T_R$
R_2	$T_{L,R}$	$y_L^{R_2\mu t} c_L$	$y_R^{R_2\mu t} c_R - y_R^{R_2\mu T} s_R$	$y_L^{R_2\mu t} s_L$	$y_R^{R_2\mu t} s_R + y_R^{R_2\mu T} c_R$
	$(X,T)_{L,R}$	$y_L^{R_2\mu t} c_L$	$y_R^{R_2\mu t} c_R$	$y_L^{R_2\mu t} s_L$	$y_R^{R_2\mu t} s_R$
	$(T,B)_{L,R}$	$y_L^{R_2\mu t} c_L - y_L^{R_2\mu T} s_L$	$y_R^{R_2\mu t} c_R$	$y_L^{R_2\mu t} s_L + y_L^{R_2\mu T} c_L$	$y_R^{R_2\mu t} s_R$
	$(X,T,B)_{L,R}$	$y_L^{R_2\mu t} c_L$	$y_R^{R_2\mu t} c_R - y_R^{R_2\mu T} s_R$	$y_L^{R_2\mu t} s_L$	$y_R^{R_2\mu t} s_R + y_R^{R_2\mu T} c_R$
	$(T,B,Y)_{L,R}$	$y_L^{R_2\mu t} c_L$	$y_R^{R_2\mu t} c_R$	$y_L^{R_2\mu t} s_L$	$y_R^{R_2\mu t} s_R$
LQ	VLQ	$\overline{\mu_R}(t_R)^C$	$\overline{\mu_L}(t_L)^C$	$\overline{\mu_R}(T_R)^C$	$\overline{\mu_L}(T_L)^C$
S_1	$T_{L,R}$	$y_L^{S_1\mu t} c_R - y_L^{S_1\mu T} s_R$	$y_R^{S_1\mu t} c_L$	$y_L^{S_1\mu t} s_R + y_L^{S_1\mu T} c_R$	$y_R^{S_1\mu t} s_L$
	$(X,T)_{L,R}$	$y_L^{S_1\mu t} c_R$	$y_R^{S_1\mu t} c_L$	$y_L^{S_1\mu t} s_R$	$y_R^{S_1\mu t} s_L$
	$(T,B)_{L,R}$	$y_L^{S_1\mu t} c_R$	$y_R^{S_1\mu t} c_L - y_R^{S_1\mu T} s_L$	$y_L^{S_1\mu t} s_R$	$y_R^{S_1\mu t} s_L + y_R^{S_1\mu T} c_L$
	$(X,T,B)_{L,R}$	$y_L^{S_1\mu t} c_R$	$y_R^{S_1\mu t} c_L$	$y_L^{S_1\mu t} s_R$	$y_R^{S_1\mu t} s_L$
	$(T,B,Y)_{L,R}$	$y_L^{S_1\mu t} c_R$	$y_R^{S_1\mu t} c_L$	$y_L^{S_1\mu t} s_R$	$y_R^{S_1\mu t} s_L$
S_3	$(X,T,B)_{L,R}$	$-y_L^{S_3\mu T} s_R$	$y_R^{S_3\mu t} c_L$	$y_L^{S_3\mu T} c_R$	$y_R^{S_3\mu t} s_L$

Table 1: The LQ$\mu t/T$ couplings in the LQ+VLQ models.

LQ	VLQ	$\overline{\mu_R} b_L$	$\overline{\mu_L} b_R$	$\overline{\mu_R} B_L$	$\overline{\mu_L} B_R$
R_2	$T_{L,R}$	$y_L^{R_2\mu t}$	0	×	×
	$(X,T)_{L,R}$	$y_L^{R_2\mu t}$	0	×	×
	$(T,B)_{L,R}$	$y_L^{R_2\mu t} c_L^b - y_L^{R_2\mu T} s_L^b$	0	$y_L^{R_2\mu T} c_L^b + y_L^{R_2\mu t} s_L^b$	0
	$(X,T,B)_{L,R}$	$y_L^{R_2\mu t} c_L^b$	$-\sqrt{2} y_R^{R_2\mu T} s_R^b$	$y_L^{R_2\mu t} s_L^b$	$\sqrt{2} y_R^{R_2\mu T} c_R^b$
	$(T,B,Y)_{L,R}$	$y_L^{R_2\mu t} c_L^b$	0	$y_L^{R_2\mu t} s_L^b$	0
LQ	VLQ	$\overline{\mu_R}(b_R)^C$	$\overline{\mu_L}(b_L)^C$	$\overline{\mu_R}(B_R)^C$	$\overline{\mu_L}(B_L)^C$
S_1	$T_{L,R}$	0	0	×	×
	$(X,T)_{L,R}$	0	0	×	×
	$(T,B)_{L,R}$	0	0	0	0
	$(X,T,B)_{L,R}$	0	0	0	0
	$(T,B,Y)_{L,R}$	0	0	0	0
S_3	$(X,T,B)_{L,R}$	$-y_L^{S_3\mu T} s_R^b$	$\sqrt{2} y_R^{S_3\mu t} c_L^b$	$y_L^{S_3\mu T} c_R^b$	$\sqrt{2} y_R^{S_3\mu t} s_L^b$

Table 2: The LQ$\mu b/B$ couplings in the LQ+VLQ models. The symbol "×" means no such interactions.

The complete contributions can be obtained from our paper [4]. Of course, they are dominated by the chirally enhanced contributions, because the non-chirally enhanced contributions are suppressed by the factor $m_\mu/m_t(m_T) \leq 10^{-3}$. Considering $m_b \ll m_t \ll m_T \approx m_B$, and $s_{L,R} \ll 1$, we show the approximate formulae of Δa_μ in Tab. 3. In the $R_2 + (X,T)_{L,R}/(T,B,Y)_{L,R}$ and $S_1 + (X,T)_{L,R}/(X,T,B)_{L,R}/(T,B,Y)_{L,R}$ models, the T contributions are highly suppressed by the factor $m_t s_{L,R}^2/m_T$. In the $R_2 + T_{L,R}/(T,B)_{L,R}/(X,T,B)_{L,R}$ and $S_1 + T_{L,R}/(T,B)_{L,R}$ models, the T contributions are suppressed by the mixing angle $s_{L,R}$. In the $S_3 + (X,T,B)_{L,R}$ model, the T and B quark contributions are dominated than top by the factor m_T/m_t.

LQ	VLQ	the approximate expressions of $\Delta\overline{a_\mu}$	coupling product order of T compared to t
R_2	$T_{L,R}$	$\frac{m_T}{m_t} f_{LR}^{R_2}(m_T^2/m_{R_2}^2)\mathrm{Re}[y_R^{R_2\mu T}(y_L^{R_2\mu t})^*]s_L + (\frac{1}{4}+\log\frac{m_t^2}{m_{R_2}^2})\mathrm{Re}[y_R^{R_2\mu t}(y_L^{R_2\mu t})^*]$	s_L
	$(X,T)_{L,R}$	$\frac{m_T}{m_t} f_{LR}^{R_2}(m_T^2/m_{R_2}^2)\mathrm{Re}[y_R^{R_2\mu t}(y_L^{R_2\mu t})^*]s_L s_R + (\frac{1}{4}+\log\frac{m_t^2}{m_{R_2}^2})\mathrm{Re}[y_R^{R_2\mu t}(y_L^{R_2\mu t})^*]$	$m_t s_R^2/m_T$
	$(T,B)_{L,R}$	$\frac{m_T}{m_t} f_{LR}^{R_2}(m_T^2/m_{R_2}^2)\mathrm{Re}[y_R^{R_2\mu t}(y_L^{R_2\mu T})^*]s_R + (\frac{1}{4}+\log\frac{m_t^2}{m_{R_2}^2})\mathrm{Re}[y_R^{R_2\mu t}(y_L^{R_2\mu t})^*]$	s_R
	$(X,T,B)_{L,R}$	$\frac{m_T}{m_t}[f_{LR}^{R_2}(m_T^2/m_{R_2}^2) + 2\widetilde{f}_{LR}^{R_2}(m_T^2/m_{R_2}^2)]\cdot\mathrm{Re}[y_R^{R_2\mu T}(y_L^{R_2\mu t})^*]s_L$ $+(\frac{1}{4}+\log\frac{m_t^2}{m_{R_2}^2})\mathrm{Re}[y_R^{R_2\mu t}(y_L^{R_2\mu t})^*]$	s_L
	$(T,B,Y)_{L,R}$	$\frac{m_T}{m_t} f_{LR}^{R_2}(m_T^2/m_{R_2}^2)\mathrm{Re}[y_R^{R_2\mu t}(y_L^{R_2\mu t})^*]s_L s_R + (\frac{1}{4}+\log\frac{m_t^2}{m_{R_2}^2})\mathrm{Re}[y_R^{R_2\mu t}(y_L^{R_2\mu t})^*]$	$m_t s_L^2/m_T$
S_1	$T_{L,R}$	$\frac{m_T}{m_t} f_{LR}^{S_1}(m_T^2/m_{S_1}^2)\mathrm{Re}[y_L^{S_1\mu T}(y_R^{S_1\mu t})^*]s_L - (\frac{7}{4}+\log\frac{m_t^2}{m_{S_1}^2})\mathrm{Re}[y_L^{S_1\mu t}(y_R^{S_1\mu t})^*]$	s_L
	$(X,T)_{L,R}$	$\frac{m_T}{m_t} f_{LR}^{S_1}(m_T^2/m_{S_1}^2)\mathrm{Re}[y_L^{S_1\mu t}(y_R^{S_1\mu t})^*]s_L s_R - (\frac{7}{4}+\log\frac{m_t^2}{m_{S_1}^2})\mathrm{Re}[y_L^{S_1\mu t}(y_R^{S_1\mu t})^*]$	$m_t s_R^2/m_T$
	$(T,B)_{L,R}$	$\frac{m_T}{m_t} f_{LR}^{S_1}(m_T^2/m_{S_1}^2)\mathrm{Re}[y_L^{S_1\mu t}(y_R^{S_1\mu T})^*]s_R - (\frac{7}{4}+\log\frac{m_t^2}{m_{S_1}^2})\mathrm{Re}[y_L^{S_1\mu t}(y_R^{S_1\mu t})^*]$	s_R
	$(X,T,B)_{L,R}$	$\frac{m_T}{m_t} f_{LR}^{S_1}(m_T^2/m_{S_1}^2)\mathrm{Re}[y_L^{S_1\mu t}(y_R^{S_1\mu t})^*]s_L s_R - (\frac{7}{4}+\log\frac{m_t^2}{m_{S_1}^2})\mathrm{Re}[y_L^{S_1\mu t}(y_R^{S_1\mu t})^*]$	$m_t s_L^2/m_T$
	$(T,B,Y)_{L,R}$	$\frac{m_T}{m_t} f_{LR}^{S_1}(m_T^2/m_{S_1}^2)\mathrm{Re}[y_L^{S_1\mu t}(y_R^{S_1\mu t})^*]s_L s_R - (\frac{7}{4}+\log\frac{m_t^2}{m_{S_1}^2})\mathrm{Re}[y_L^{S_1\mu t}(y_R^{S_1\mu t})^*]$	$m_t s_L^2/m_T$
S_3	$(X,T,B)_{L,R}$	$\frac{m_T}{m_t}[f_{LR}^{S_3}(m_T^2/m_{S_3}^2) + 2\widetilde{f}_{LR}^{S_3}(m_T^2/m_{S_3}^2)]\cdot\mathrm{Re}[y_L^{S_3\mu T}(y_R^{S_3\mu t})^*]s_L$ $+(\frac{7}{4}+\log\frac{m_t^2}{m_{S_3}^2})\mathrm{Re}[y_L^{S_3\mu T}(y_R^{S_3\mu t})^*]s_R$	m_T/m_t

Table 3: In the third column, we show the approximate formulae of the Δa_μ. In the fourth column, we show the order of the multiplication of left and right-handed T LQ Yukawa couplings with respect to the top quark. In the above, we redefine Δa_μ as $m_\mu m_t \Delta\overline{a_\mu}/(4\pi^2 m_{\mathrm{LQ}}^2)$.

4. Numerical analysis

We choose the input parameters as $m_\mu = 105.66\mathrm{MeV}$, $m_b = 4.2\mathrm{GeV}$, and $m_t = 172.5\mathrm{GeV}$ [7]. For the VLQ parameters, the main constraints are from direct search [8, 9] and electro-weak precision observables [6, 10], which require the VLQ mass to be $O(\mathrm{TeV})$ and the input mixing angle to be less than 0.1. For the LQ mass, the direct search requires it to be above TeV [11, 12]. Then, we adopt the mass parameters to be $m_T = 1\mathrm{TeV}$ and $m_{\mathrm{LQ}} = 2\mathrm{TeV}$ by default. The input mixing angle is set as $s_L = 0.05$ (singlet and triplet VLQs) and $s_R = 0.05$ (doublet VLQs). In Fig. 1, we show the regions allowed at 1σ (green) and 2σ (yellow) CL, respectively.

5. LQ Phenomenology at hadron colliders

In the minimal R_2/S_1 models, the LQ decay final states are SM quark and lepton. In the LQ+VLQ models, there are new LQ decay channels. Here, we will study the $R_2^{5/3} \to t/T\mu^+$ and $S_1/S_3^{1/3} \to \bar{t}/\bar{T}\mu^+$ decay channels [2]. Considering $m_t \ll m_T$ and $s_{L,R} \ll 1$, we show the approximate expressions of $\Gamma(\mathrm{LQ} \to T\mu)/\Gamma(\mathrm{LQ} \to t\mu)$ in Tab. 4. Then, we find that the $T\mu$ decay channel is important in the $R_2 + T_{L,R}/(T,B)_{L,R}/(X,T,B)_{L,R}$, $S_1 + T_{L,R}/(T,B)_{L,R}$, and

[2]For the other LQs, the decay channels can be $R_2^{2/3} \to b/B\mu^+$, $S_3^{4/3} \to \bar{b}/\bar{B}\mu^+$, and $S_3^{-2/3} \to \bar{X}\mu^+$.

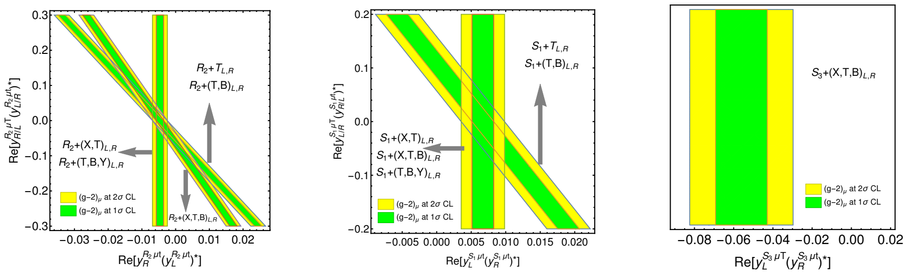

Figure 1: The allowed region in the plane of $\mathrm{Re}[y^{R_2\mu T}_{R/L}(y^{R_2\mu t}_{L/R})^*]$ – $\mathrm{Re}[y^{R_2\mu t}_{R}(y^{R_2\mu t}_{L})^*]$ (left, R_2 + VLQ) and $\mathrm{Re}[y^{S_1\mu T}_{L/R}(y^{S_1\mu t}_{R/L})^*]$ – $\mathrm{Re}[y^{S_1\mu t}_{L}(y^{S_1\mu t}_{R})^*]$ (middle, S_1 + VLQ). The right is for the $S_3 + (X,T,B)_{L,R}$ model.

$S_3 + (X,T,B)_{L,R}$ models. For the LQ production, there are pair, single, and off-shell channels.

LQ	VLQ	the approximate expressions of $\Gamma(\mathrm{LQ}\to T\mu)/\Gamma(\mathrm{LQ}\to t\mu)$	suppress or not
R_2	$T_{L,R}$	$(1-\frac{m_T^2}{m_{R_2}^2})^2\lvert y_R^{R_2\mu T}\rvert^2/(\lvert y_L^{R_2\mu t}\rvert^2+\lvert y_R^{R_2\mu t}\rvert^2)$	No
	$(X,T)_{L,R}$	$(1-\frac{m_T^2}{m_{R_2}^2})^2\lvert y_R^{R_2\mu t}\rvert^2 s_R^2/(\lvert y_L^{R_2\mu t}\rvert^2+\lvert y_R^{R_2\mu t}\rvert^2)$	s_R^2
	$(T,B)_{L,R}$	$(1-\frac{m_T^2}{m_{R_2}^2})^2\lvert y_L^{R_2\mu T}\rvert^2/(\lvert y_L^{R_2\mu t}\rvert^2+\lvert y_R^{R_2\mu t}\rvert^2)$	No
	$(X,T,B)_{L,R}$	$(1-\frac{m_T^2}{m_{R_2}^2})^2\lvert y_R^{R_2\mu T}\rvert^2/(\lvert y_L^{R_2\mu t}\rvert^2+\lvert y_R^{R_2\mu t}\rvert^2)$	No
	$(T,B,Y)_{L,R}$	$(1-\frac{m_T^2}{m_{R_2}^2})^2\lvert y_L^{R_2\mu t}\rvert^2 s_L^2/(\lvert y_L^{R_2\mu t}\rvert^2+\lvert y_R^{R_2\mu t}\rvert^2)$	s_L^2
S_1	$T_{L,R}$	$(1-\frac{m_T^2}{m_{S_1}^2})^2\lvert y_L^{S_1\mu T}\rvert^2/(\lvert y_L^{S_1\mu t}\rvert^2+\lvert y_R^{S_1\mu t}\rvert^2)$	No
	$(X,T)_{L,R}$	$(1-\frac{m_T^2}{m_{S_1}^2})^2\lvert y_L^{S_1\mu t}\rvert^2 s_R^2/(\lvert y_L^{S_1\mu t}\rvert^2+\lvert y_R^{S_1\mu t}\rvert^2)$	s_R^2
	$(T,B)_{L,R}$	$(1-\frac{m_T^2}{m_{S_1}^2})^2\lvert y_R^{S_1\mu T}\rvert^2/(\lvert y_L^{S_1\mu t}\rvert^2+\lvert y_R^{S_1\mu t}\rvert^2)$	No
	$(X,T,B)_{L,R}$	$(1-\frac{m_T^2}{m_{S_1}^2})^2\lvert y_R^{S_1\mu t}\rvert^2 s_L^2/(\lvert y_L^{S_1\mu t}\rvert^2+\lvert y_R^{S_1\mu t}\rvert^2)$	s_L^2
	$(T,B,Y)_{L,R}$	$(1-\frac{m_T^2}{m_{S_1}^2})^2\lvert y_R^{S_1\mu t}\rvert^2 s_L^2/(\lvert y_L^{S_1\mu t}\rvert^2+\lvert y_R^{S_1\mu t}\rvert^2)$	s_L^2
S_3	$(X,T,B)_{L,R}$	$(1-\frac{m_T^2}{m_{S_3}^2})^2\lvert y_L^{S_3\mu T}\rvert^2/\lvert y_R^{S_3\mu t}\rvert^2$	No

Table 4: In the third column, we list the approximate formulae of $T\mu$ partial decay width over $t\mu$ in the LQ+VLQ models. In the fourth column, we show the order of $\Gamma(\mathrm{LQ}\to T\mu)$ compared to the $\Gamma(\mathrm{LQ}\to t\mu)$.

What is more, the T quark can decay into the bW, tZ, th final states further. Thus, it will lead to the characteristic multi-top and multi-muon signals at hadron colliders.

6. Summary and conclusions

We explain the $(g-2)_\mu$ anomaly in the LQ and VLQ extended models. In the $R_2 + (X,T)_{L,R}/(T,B,Y)_{L,R}$ and $S_1 + (X,T)_{L,R}/(X,T,B)_{L,R}/(T,B,Y)_{L,R}$ models, it is dominated by the top quark contributions. In the $R_2 + T_{L,R}/(T,B)_{L,R}/(X,T,B)_{L,R}$ and $S_1 + T_{L,R}/(T,B)_{L,R}$ models, both the top and T quark contributions are important. In the $S_3 + (X,T,B)_{L,R}$ model, it is dominated by the T and B quark contributions. In addition to the conventional $t\mu$ decay channel, the LQ can also decay into $T\mu$ final states, which can become important in the $R_2 + T_{L,R}/(T,B)_{L,R}/(X,T,B)_{L,R}$, $S_1 + T_{L,R}/(T,B)_{L,R}$ models, and $S_3 + (X,T,B)_{L,R}$ models.

Acknowledgments

This research was supported by an appointment to the Young Scientist Training Program at the APCTP through the Science and Technology Promotion Fund and Lottery Fund of the Korean Government. This was also supported by the Korean Local Governments-Gyeongsangbuk-do Province and Pohang City.

References

[1] T. Aoyama et al. The anomalous magnetic moment of the muon in the Standard Model. *Phys. Rept.*, 887:1–166, 2020.

[2] G. W. Bennett et al. Final Report of the Muon E821 Anomalous Magnetic Moment Measurement at BNL. *Phys. Rev. D*, 73:072003, 2006.

[3] B. Abi et al. Measurement of the Positive Muon Anomalous Magnetic Moment to 0.46 ppm. *Phys. Rev. Lett.*, 126(14):141801, 2021.

[4] Shi-Ping He. Leptoquark and vectorlike quark extended models as the explanation of the muon $g-2$ anomaly. *Phys. Rev. D*, 105(3):035017, 2022. [Erratum: Phys.Rev.D 106, 039901 (2022)].

[5] I. Doršner, S. Fajfer, A. Greljo, J. F. Kamenik, and N. Košnik. Physics of leptoquarks in precision experiments and at particle colliders. *Phys. Rept.*, 641:1–68, 2016.

[6] J. A. Aguilar-Saavedra, R. Benbrik, S. Heinemeyer, and M. Pérez-Victoria. Handbook of vectorlike quarks: Mixing and single production. *Phys. Rev. D*, 88(9):094010, 2013.

[7] P. A. Zyla et al. Review of Particle Physics. *PTEP*, 2020(8):083C01, 2020.

[8] Albert M Sirunyan et al. Search for vector-like quarks in events with two oppositely charged leptons and jets in proton-proton collisions at $\sqrt{s} = 13$ TeV. *Eur. Phys. J. C*, 79(4):364, 2019.

[9] Morad Aaboud et al. Combination of the searches for pair-produced vector-like partners of the third-generation quarks at $\sqrt{s} = 13$ TeV with the ATLAS detector. *Phys. Rev. Lett.*, 121(21):211801, 2018.

[10] Chien-Yi Chen, S. Dawson, and Elisabetta Furlan. Vectorlike fermions and Higgs effective field theory revisited. *Phys. Rev. D*, 96(1):015006, 2017.

[11] Albert M Sirunyan et al. Search for leptoquarks coupled to third-generation quarks in proton-proton collisions at $\sqrt{s} = 13$ TeV. *Phys. Rev. Lett.*, 121(24):241802, 2018.

[12] Georges Aad et al. Search for pair production of scalar leptoquarks decaying into first- or second-generation leptons and top quarks in proton–proton collisions at $\sqrt{s} = 13$ TeV with the ATLAS detector. *Eur. Phys. J. C*, 81(4):313, 2021.